The flow due to a two-dimensional jet issuing parallel to a flat plate

By R. A. SAWYER
Engineering Department, Cambridge University

(Received 17 May 1960)

An experiment has been performed to determine the cavity pressure and cavity length for the flow under a curved two-dimensional turbulent jet discharging parallel to a flat plate at some distance from the surface. The measurements agree quite closely with the predictions of a simple analysis of the flow when a value is assigned to the spread parameter for the curved jet which is somewhat different from that for the plane jet.

Detailed pressure and velocity measurements show that the rate of growth of the curved jet is in fact closely similar to that of the plane jet. This suggests that the adjustment of the spread parameter should be regarded simply as a convenient device for taking into account the quantitative errors of the assumptions made in the analysis.

1. Introduction

This work was undertaken to give some experimental backing to a simple model proposed by Dodds (1960) for the flow resulting from a two-dimensional jet issuing parallel to a flat plate. Recently it has come to the author's notice that a similar experiment has been performed by Bourque (1959). However, the two sets of results appear to be complementary rather than duplicative in that they cover somewhat different ranges of the relevant variables.

The essential feature of the flow is the entrainment of fluid by the turbulent jet, which enables a stable flow pattern to be attained by the following mechanism. The entrainment of fluid near to the plate causes a pressure difference across the jet, curving the jet towards the plate. The jet divides on striking the plate, a proportion of the volume flow being reversed into the cavity. The final configuration is that in which the mean volume flow entrained from the cavity by the inner edge of the jet is balanced by the mean volume flow fed back into the cavity at the attachment point of the jet to the plate.

This flow is typical of cavity flows, other examples of which are to be found in connexion with separation bubbles, sudden expansions in pipes and channels, the flow over spoilers, the wakes of bluff bodies at certain Reynolds numbers, and so on.

It is well recognized (for example, see Townsend 1956) that the mechanism of entrainment is intimately connected with the growth of turbulent shear flows, and it is possible to use entrainment properties in the setting up of mean flow equations for such flows. For example, it is possible to construct an entrainment

relation for the turbulent boundary layer under the assumption that the entrainment properties at a particular boundary-layer station are a function of the shape of the velocity profile there as given, say, by the shape parameter $H = \delta^*/\theta$ (in the notation of Ludwieg & Tillman 1951). A detailed experiment could be performed to relate an entrainment parameter to H and R_0 which, with the Ludwieg–Tillman (1951) relations connecting C_f, R_θ and H, would furnish an approximate method for the calculation of turbulent boundary layers through the momentum and entrainment equations. This idea has been put forward by Head (1958).

Implicit in such arguments is the assumption that the turbulent structure of a shear layer, or that part of the turbulent structure which affects the mechanism of entrainment, is a function of an over-all shape parameter. In the case of a plane turbulent jet or other free turbulent shear layer, it is expected that the entrainment properties will be completely dependent on profile shape, because of a lack of solid boundaries. Turbulent shear flows may be considered to consist of a body of wholly turbulent fluid separated from the non-turbulent fluid by a clearly defined surface (the 'laminar superlayer' introduced by Corrsin & Kistler (1954) of an irregular and fluctuating character. The process of entrainment may be taken to be the advancing of this bounding surface into the non-turbulent fluid. Townsend indicates that the position of the bounding surface of the turbulent fluid is almost wholly due to the large eddy structure of the flow, which is the structure responsible for the value of the shape parameter H of the velocity profile.

The entrainment properties of a curved two-dimensional turbulent jet are expected to differ from those of the corresponding plane jet, momentum transport arguments indicating a reduced entrainment along the inner edge and an enhanced entrainment along the outer edge. For consider the transport of a small parcel of fluid from a region of higher velocity to a region of lower velocity nearer to the outside edge of the jet. If this parcel of fluid arrives with some excess velocity over its surroundings, it is now subjected to a greater centrifugal force than its surroundings. But its surroundings are subjected to centrifugal forces and pressure forces which just balance in the mean. Thus it is expected that the parcel of fluid will experience a total force tending to move it further outwards, which implies a more vigorous mixing than that which occurs with no curvature. A reverse argument holds for the mixing at the inner edge.

Dodds has put forward a simple model of the cavity flows of a curved two-dimensional reattaching jet, in which plausible assumptions regarding the division of the jet at reattachment lead to expressions relating the cavity pressure and cavity length to the jet momentum per unit jet width and the geometry of the boundaries. These expressions involve a spread parameter connected with the entrainment properties of the inner edge of the jet. The experiment has been performed to ascertain the correctness of Dodds's predictions and to find the value of the spread parameter.

2. Notation

h distance of slot centre-line from plate;
h_0 height of equivalent control volume used in reversed flow pressure recovery calculation;
J jet momentum/unit span;
J_2 momentum/unit span of reversed flow;
J_3 momentum/unit span of flow downstream of reattachment;
$K = 1{\cdot}825/\sigma$;
l cavity length, or distance of reattachment point from step;
p static pressure;
p_a static pressure far downstream;
p_s an average static pressure inside the cavity;
Δp pressure difference across jet;
Δp_2 pressure recovery of reversed flow;
Q quantity flow/unit span in jet;
Q_2 quantity flow/unit span in initial reversed flow;
R radius of curvature of jet;
t thickness of jet at exit;
$T = \tanh \eta_R$;
T_1 value of T at X_1;
u mean velocity;
U_0 reference velocity;
$U_{\max}$ maximum velocity of jet profile;
x, y co-ordinates parallel and perpendicular to plate ($x = 0$ at step, $y = 0$ at plate);
X, Y co-ordinates along and perpendicular to jet centre-line ($X = X_0$ at slot, $Y = 0$ on jet centre line);
X_1 value of X where jet inner edge would touch plate;
δ_1 thickness of jet at X_1;
δ_2, δ_3 thicknesses of initial reversed flow and initial downstream flow at the reattachment point;
μ viscosity;
ψ streamline parameter ($\psi = 0$ on reattaching streamline);
ρ density;
σ spread parameter ($= 7{\cdot}67$ for plane jet);
θ angle between jet centre-line at X_1 and plate;
$\eta = \sigma Y/X$, non-dimensional jet profile co-ordinate;
η_R value of η on reattaching streamline.

The notation is further explained by figure 1.

3. Dimensional analysis

The significant variables of the problem are the step-height h, the slot thickness t, a velocity U_0 representative of the jet velocity at the slot and the fluid properties μ and ρ. If these quantities are specified, the physical features of the flow are determined.

Dimensional considerations then show that the cavity length and the pressure difference across the jet may be expressed as follows:

$$\frac{l}{h} = f_1\left(\frac{h}{t}, \frac{\rho U_0 t}{\mu}\right),$$

where U_0 is given by $J = \rho U_0^2 t$, the jet momentum/unit span, and

$$\frac{p_s - p_a}{\frac{1}{2}\rho U_0^2} = f_2\left(\frac{h}{t}, \frac{\rho U_0 t}{\mu}\right).$$

In particular, if the jet is thin (h/t large) and fully turbulent ($\rho U_0 t/\mu$ large), it is expected that

$$\frac{\Delta p}{J/h} = -\frac{(p_s - p_a)h}{\rho U_0^2 t}$$

should be nearly independent of $\rho U_0 t/\mu$ (or $\sqrt{(J\rho t)}/\mu$) and substantially independent of h/t.

Similarly, l/h is expected to be nearly independent of jet Reynolds number and to vary little with h/t for large h/t.

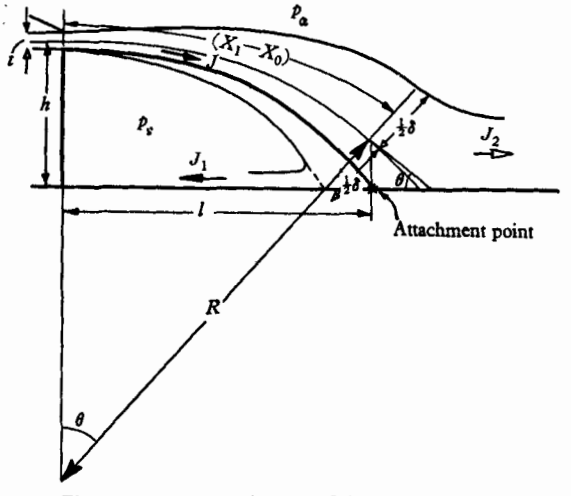

FIGURE 1. Notation used in the analysis.

4. An approximate analysis for the case of a thin fully developed turbulent jet

The analysis runs as follows. The curvature of the jet is expressed as the ratio of the pressure difference across the jet to the jet momentum. Knowing the geometry of the jet centre-line, assumptions regarding the jet velocity profile and rate of spread (as measured by a spread parameter σ) lead to an expression for the amount of air entrained by the jet along its inner edge, which is taken to be the volume flow fed back into the cavity at reattachment. Thus the division of volume flow of the jet at reattachment is known. Assumptions of velocity profile shapes of the initial reversed flow and the initial attached downstream flow, with the aid of a momentum balance equation at the reattachment point,

then give the division of momentum flow at reattachment. But the division of momentum at reattachment implies the geometry of the jet. Thus the chain of reasoning is complete and a solution can be found. The analysis is set out in detail below.

Assume that the velocity profile of the jet is similar to that of a two-dimensional plane jet, so that the profile is given approximately by the equation

$$\frac{u}{U_{\max}} = \operatorname{sech}^2 \eta,$$

where $\eta = \sigma Y/X$ (Görtler 1942), and where X, Y are co-ordinates measuring distances along and perpendicular to the jet centre-line. Note that $X = 0$ does not coincide with the position of the slot.

The value of the free constant σ for the case of the plane jet was found experimentally by Reichardt (1942) to be 7·67. It is expected that the value of σ relevant to entrainment along the inner edge of the curved jet will be somewhat higher than this due to suppression of turbulent mixing as a consequence of curvature.

The jet momentum per unit span is given by

$$J = \tfrac{4}{3}\rho U_{\max}^2 \frac{X}{\sigma},$$

and the volume flow per unit span is given by

$$Q = 2U_{\max}\frac{X}{\sigma}.$$

Thus
$$Q = \sqrt{\left(\frac{3JX}{\sigma\rho}\right)} \quad \text{and} \quad U_{\max} = \sqrt{\left(\frac{3\sigma J}{4\rho X}\right)}. \tag{1}$$

It is assumed that there is a constant pressure p_s in the cavity, so that there is a constant pressure difference $\Delta p = (p_a - p_s)$ acting across the jet. If the jet is thin, the centre-line of the jet lies approximately on an arc of a circle of radius R, where

$$\Delta p = \frac{J}{R}. \tag{2}$$

In the absence of any precise guide, the station $X = X_1$, which is representative of the state of the jet near the reattachment point, is taken to be that at which the inner edge of the jet as given by $u/U_{\max} = 0{\cdot}1$ would first strike the plate, i.e. in such a position that, in the absence of reattachment-point effects, the jet centre-line continues to lie along the circle of radius R and the jet continues to grow at its normal rate, the locus $u/U_{\max} = 0{\cdot}1$ intersects the line of the plate.

Then the thickness δ_1 of the jet at $X = X_1$ is given by

$$\frac{\delta_1}{2X_1} = \frac{1}{\sigma}\tanh^{-1}\sqrt{(0{\cdot}9)}$$

$$= \frac{1{\cdot}825}{\sigma} = K, \quad \text{say.} \tag{3}$$

Geometrically it is seen that

$$X_1 - X_0 = R\theta, \tag{4}$$

where θ is the angle between the jet centre-line at station $X = X_1$ and the plate, and where $X = X_0$ corresponds to the slot. We also have

$$h = R(1-\cos\theta)+\tfrac{1}{2}\delta_1\cos\theta, \tag{5}$$

and for ease of computation take

$$l = R\sin\theta. \tag{6}$$

The mass flow between the jet centre-line and the reattaching streamline (the streamline springing from the inner edge of the slot) is constant and equal to $\frac{1}{2}\sqrt{(Jtp)}$, assuming a uniform velocity profile across the slot.

Thus the reattaching streamline is given by

$$\begin{aligned}\tfrac{1}{2}\sqrt{(Jtp)} &= \rho\sqrt{\left(\frac{3J\sigma}{4\rho X}\right)}\frac{X}{\sigma}\int_0^{\eta_R}\operatorname{sech}^2\eta\,d\eta \\ &= \sqrt{\left(\frac{3\rho JX}{4\sigma}\right)}T,\end{aligned}$$

where $T = \tanh\eta_R$ corresponds to the value of η at the reattaching streamline, i.e.

$$\frac{1}{T^2} = \frac{3X}{\sigma t}. \tag{7}$$

In particular, we have

$$X_0 = \frac{\sigma t}{3}, \tag{8}$$

$$\frac{X_0}{X_1} = T_1^2. \tag{9}$$

Equations (1) to (9) give

$$\frac{h}{t} = \frac{\sigma}{3\theta}\left(\frac{1-T_1^2}{T_1^2}\right)\left(1-\cos\theta+\frac{K\theta\cos\theta}{1-T_1^2}\right), \tag{10}$$

$$\frac{l}{h} = \frac{\sin\theta}{\{1-\cos\theta+K\theta\cos\theta/(1-T_1^2)\}}, \tag{11}$$

$$\frac{\Delta p}{J/h} = \{1-\cos\theta+K\theta\cos\theta/(1-T_1^2)\}. \tag{12}$$

To relate T_1 to θ, consider the momentum balance at the reattachment point. Dodds supposes that the initial reversed flow and initial downstream flow have velocity profiles similar to that of half a Görtler jet profile with maximum velocities $U_{\max_1}\sin\theta$ and $U_{\max_1}$, respectively. The factor $\sin\theta$ is arbitrary, being chosen to satisfy the conditions for $\theta = 0, \frac{1}{2}\pi$. Any reasonably well-behaved function $f(\theta)$ such that $f(\theta) = 0, f(\frac{1}{2}\pi) = 1$ would be equally acceptable. $U_{\max_1}$ is the velocity maximum of the free-jet profile at $X = X_1$.

If δ_2, δ_3 are the thicknesses of half-jet profiles, the equations of continuity and momentum in the x-direction at the reattachment point give

$$\begin{aligned}\delta_1 &= \delta_2\sin\theta+\delta_3, \\ \delta_1\cos\theta &= -\delta_2\sin^2\theta+\delta_3,\end{aligned}$$

if pressure differences are neglected near the attachment point, so that

$$\frac{\delta_2}{\delta_1} = \frac{1}{\sin\theta}\left(\frac{1-\cos\theta}{1+\sin\theta}\right).$$

Thus the reversed volume flow is

$$U_{\max_1}\sin\theta\frac{\delta_2}{\sigma K}\int_0^\infty \operatorname{sech}^2\eta\,d\eta = U_{\max_1}\frac{\delta_1}{\sigma K}\left(\frac{1-\cos\theta}{1+\sin\theta}\right)$$
$$= \sqrt{\left(\frac{3\sigma J}{4\rho X_1}\right)}\frac{\delta_1}{\sigma K}\left(\frac{1-\cos\theta}{1+\sin\theta}\right),$$

from (1). But this is equal to

$$\tfrac{1}{2}(Q_1-Q_0) = \frac{1}{2}\left\{\sqrt{\left(\frac{3JX_1}{\sigma\rho}\right)}-\sqrt{\left(\frac{3JX_0}{\sigma\rho}\right)}\right\}.$$

Hence

$$\frac{\delta_1}{KX_1}\left(\frac{1-\cos\theta}{1+\sin\theta}\right) = 1-\sqrt{\frac{X_0}{X_1}},$$

or

$$T_1 = 1-2\left(\frac{1-\cos\theta}{1+\sin\theta}\right). \tag{13}$$

Bourque (1959) has obtained a different relation between T_1 and θ by the following reasoning. Assume that at the attachment point the jet flow divides in such a manner that the profiles of the initial reversed flow and initial flow downstream of the attachment point are similar to the parts of the free-jet profile at $X = X_1$ below and above the reattaching streamline, at least in so far as over-all volume flow and momentum are concerned.

Then the momentum per unit span of the jet below the reattaching streamline is

$$J_2 = \int_{T_1}^1 \rho U_{\max_1}^2\frac{X_1}{\sigma}(1-T^2)\,dT$$
$$= \tfrac{3}{4}J(\tfrac{2}{3}-T_1+\tfrac{1}{3}T_1^3).$$

The momentum per unit span of the jet above the reattaching streamline is

$$J_3 = \int_{-1}^{T_1}\rho U_{\max_1}^2\frac{X_1}{\sigma}(1-T^2)\,dT$$
$$= \tfrac{3}{4}J(\tfrac{2}{3}+T_1-\tfrac{1}{3}T_1^3).$$

If pressure differences near the attachment point are neglected, the momentum balance at the attachment point gives

$$J\cos\theta = J_3-J_2,$$

so that

$$\cos\theta = \tfrac{3}{2}T_1-\tfrac{1}{2}T_1^3. \tag{14}$$

Relation (14) is likely to be more accurate than relation (13), and accordingly the experimental results have been compared with the predictions given by equations (10), (11), (12) and (14).

5. Experimental arrangement

The experimental arrangement is shown in figure 2. The top of the tank was bolted down through a rectangular spacer, one side of which formed the lower surface of the slot and the step on the plate. Three step heights were used, namely $\frac{1}{2}$, 1 and 2 in. The upper surface of the slot was attached to the top of the

tank by horizontal bolts through slotted holes so that the width of the slot was variable between zero and $\frac{1}{4}$ in. The combination of step heights and slot widths covered a large range of h/t.

A fine-mesh gauze was placed across the pipe from the blower at the entry to the tank so as to smooth the flow from the blower.

Vertical end-plates isolating 12 in. of the slot flow were fixed to the plate to preserve two-dimensional conditions as far as possible, in particular to remove spanwise flow into the low-pressure cavity. It was found that the flow was substantially two-dimensional (see below).

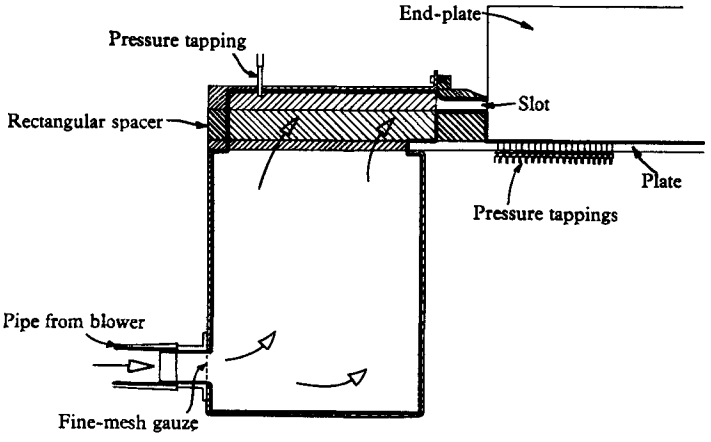

FIGURE 2. Experimental arrangement.

The static pressure distribution on the plate was measured by means of surface pressure tappings at intervals of 0·2 in. Static pressures and total pressures were measured by means of static and Pitot tubes fixed to a vertical traverse gear sliding on a spanwise horizontal bar which moved on streamwise horizontal rails. The jet momentum was found from Pitot and static traverses across the slot. All pressure readings were referred to a pressure tapping in the top of the tank.

Tests of two-dimensionality

Velocity traverses across the slot showed that the maximum velocity at the slot was constant across the slot length to 1 %. The surface streamlines on the plate and end-plates were made visible by applying a suspension of titanium dioxide in penetrating oil to these surfaces which had been painted matt black. Figure 3 (plate 1) shows that the streamlines on the end plates are not at all similar to the mean streamlines in figure 4, and that the reattachment distance varies somewhat along the width of the plate. The photographs indicate that there is a secondary flow close to the end-plates which feeds air from outside into the cavity. Thus there is not an exact balance between the quantity of air entrained by the jet from the cavity and the quantity of reversed flow at reattachment. Near the centre of the slot length, however, it is estimated that this lack of balance is negligible and that the flow corresponds very nearly to two-dimensional conditions.

Pressure readings and measurements of reattachment distance

Detailed measurements of mean velocities and reattachment position were carried out for the slot width and step height giving the case $h/t = 5{\cdot}62$.

Because of the end effects described above, it was not possible to use static pressure tappings in an end-plate to give a reliable static pressure map of the cavity. Apart from the pressures measured by means of tappings in the horizontal plate, all static pressures were measured by a standard static tube aligned

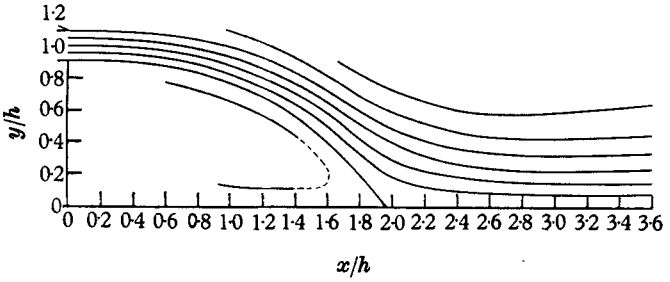

FIGURE 4. Streamlines for case $h/t = 5{\cdot}62$.

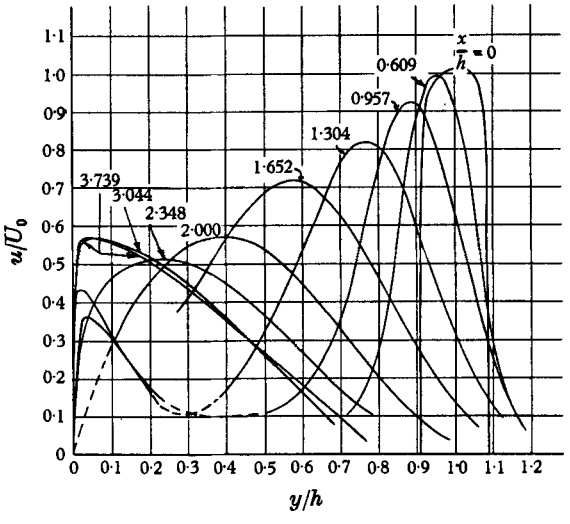

FIGURE 5. Velocity profiles for case $h/t = 5{\cdot}62$.

with the direction of local streamlines. Because of the sensitivity of flattened Pitot tubes in regions of strong turbulence to the fluctuations of flow direction all total pressures (other than those of the reversed flow regions), were measured by a round thin-wall Pitot tube of diameter 0·040 in. aligned with the mean flow direction. This Pitot tube was insensitive to yaw to $\frac{1}{2}\%$ of dynamic pressure over the range $\pm 15°$. Total pressures in the reversed flow near to the plate, i.e. in those reversed flow regions in which the fluctuations of flow direction were suppressed by the proximity of the plate, were measured with a flattened Pitot tube of 0·010 in. over-all thickness.

The technique used was to make transverses with the tubes at various angles, selecting those which gave stationary values of static pressure and Pitot pressure with respect to alignment angle at the point considered. The velocity profiles obtained (figure 5), together with approximate flow directions, gave a mean streamline picture from which more accurate flow directions were found. Using these new flow directions a more accurate streamline picture was calculated, and so on. As a check on the final streamline plot (figure 4) obtained by repeating the above procedure three times, it was seen that the position of reattachment calculated from the integrated velocity profiles corresponded very closely (l/h accurate to 1 %) to that found by surface-Pitot traverses and to that indicated by the visualization technique. The surface-Pitot traverses were made with identical flattened Pitots, one facing forward and one reversed. The results are presented in table 1. The reattachment point was taken as that point at which the

x/h	$\frac{P-p_a}{\frac{1}{2}\rho U_0^2}$, forward Pitot	$\frac{P-p_a}{\frac{1}{2}\rho U_0^2}$, reversed Pitot
1·826	0·540	0·415
1·913	0·585	0·550
2·000	0·600	0·625

TABLE 1. Attachment point determined by surface Pitots. For case $h/t = 5{\cdot}62$.

two Pitots gave the same reading. It was found that the position of reattachment coincided with the position of maximum pressure on the horizontal plate. This position of maximum pressure was taken as the reattachment position in all other cases.

In calculating the velocity profiles from Pitot and static traverses the Young & Maas (1936) correction to Pitot measurements was applied. Even in the case of extreme velocity gradients encountered at the slot itself, the Young & Maas correction applied to the 0·040 in. Pitot gave profile widths accurate to 0·001 in. as measured by slot width. One particular profile at the slot obtained in this way was checked against that measured with a flattened boundary-layer Pitot of 0·010 in. over-all thickness and the two were found to be almost identical.

6. Comparison of experimental results with the analysis

The values of $\Delta p/(J/h)$ and l/h obtained for various h/t are given in table 2, and the results found by Bourque in the range of h/t considered are given for comparison in table 3. In figures 6 and 7 these results are compared with corresponding theoretical curves for $\sigma = 5$, 10, 15 and 20. It is interesting to see that the dual-jet flow measurements of Miller & Comings (1960) give values of $\Delta p/(J/h)$ and l/h which agree quite well with the results presented here.

As mentioned previously, the position of reattachment was taken to be the position of maximum pressure on the plate. Figure 8 shows the distribution of pressure on the plate. It is seen that for large h/t the pressure is far from uniform through the cavity. However, figure 9 shows that the pressure along the plate

follows quite closely the static pressure under the jet, and the value of Δp chosen was the (negative) mean of the pressure on the plate over the range of x/h between zero and 0·95 times its value at $p - p_a = 0$.

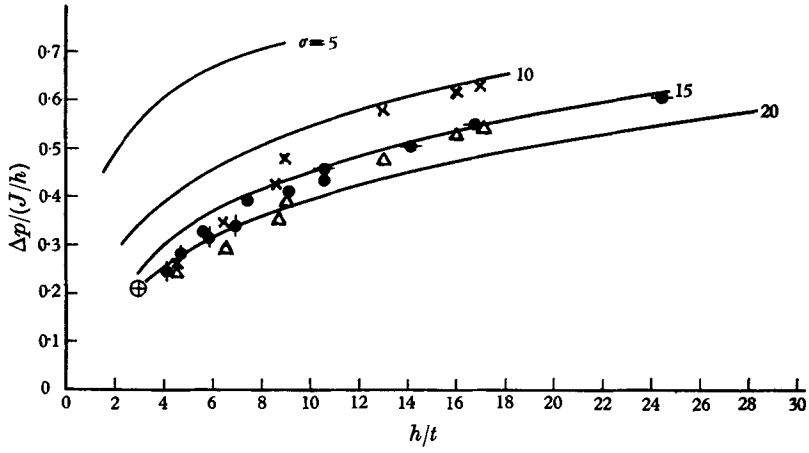

FIGURE 6. Variation of $\Delta p/(J/h)$ with h/t compared with Dodds–Bourque analysis. ⊕, Miller & Comings dual-jet flow; ϕ, ½ in. step; ●, 1 in. step; -●-, 2 in. step; ×, Bourque's results (using pressure minimum on plate to define Δp); △, Bourque's results (recalculated to correspond to average Δp and corrected J).

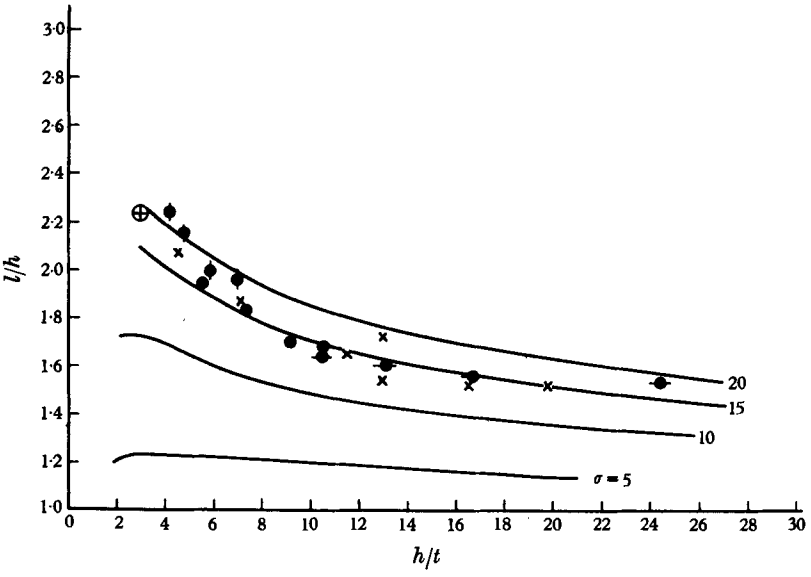

FIGURE 7. Variation of l/h with h/t compared with the analysis. ϕ, ½ in. step; ●, 1 in. step; -●-, 2 in. step; ×, Borque's results; ⊕, Miller & Comings dual-jet flow.

It is seen that Bourque's results giving the variation of l/h with h/t agree very well with those obtained by the author. However, there is considerable systematic discrepancy between the sets of results for the variation of $\Delta p/(J/h)$ with h/t.

Bourque uses a very short entry length to the jet exit in order to obtain a square-edged initial jet profile and computes the jet momentum J from the

measured pressure in the chamber just before the contraction to the slot under the assumption that the dynamic pressure of the jet is that given by the chamber pressure. However, Bourque also presents measurements of the initial jet profiles which show that the velocity is far from uniform across the slot width.

For comparison, the values of $\Delta p/(J/h)$ measured by Bourque and computed using the minimum static pressure on one plate in his definition of Δp and the chamber pressure to define J, have been recalculated using the definitions of Δp and J used in this experiment.

	h/t	l/h	$\Delta p/(J/h)$
$\frac{1}{2}$ in. step	4·15	2·25	0·244
	4·81	2·15	0·279
	5·92	2·00	0·318
	6·99	1·97	0·342
1 in. step	5·62	1·96	0·327
	7·35	1·83	0·394
	9·13	1·70	0·412
	10·64	1·68	0·439
2 in. step	10·65	1·65	0·459
	14·06	1·60	0·508
	16·74	1·57	0·556
	24·40	1·54	0·606

TABLE 2. Experimental results.

h/t	$\Delta p/(J/h)$*	h/t	l/h
4·5	0·27	4·5	2·07
6·5	0·35	7·1	1·87
8·7	0·43	11·5	1·65
9·0	0·48	13·0	1·54
13	0·58	13·0	1·72
16	0·62	16·5	1·52
17	0·61	19·8	1·52

* Note that Bourque takes pressure minimum on plate to define Δp.

TABLE 3. Bourque's results.

In this connexion it should be noted that while in the present experiment the jet Reynolds number $\sqrt{(J\rho t)}/\mu$ was almost constant for all readings at about $9{\cdot}5 \times 10^4$, Bourque's experiment was conducted at much lower Reynolds numbers between $0{\cdot}8 \times 10^4$ and $1{\cdot}5 \times 10^4$.

Figures 6 and 7 show that $\Delta p/(J/h)$ and l/h are quite closely defined functions of h/t following roughly the curves given by the analysis for $\sigma = 15$.

7. Discussion of detailed velocity and pressure measurements

Velocity profiles across sections at right angles to the jet have been calculated for the stations $x/h = 0{\cdot}609$ and $x/h = 1{\cdot}304$ (referring to the position of the velocity maximum of the profile) for the case $h/t = 5{\cdot}62$, by a direct application

of the assumption that the local growth of the jet is that of the free jet with spread parameter $\sigma = 15$ to the measured velocity profiles at $x/h = 0{\cdot}609$ and $x/h = 1{\cdot}304$. These profiles are shown in figure 10. The method of calculation is set out in an appendix.

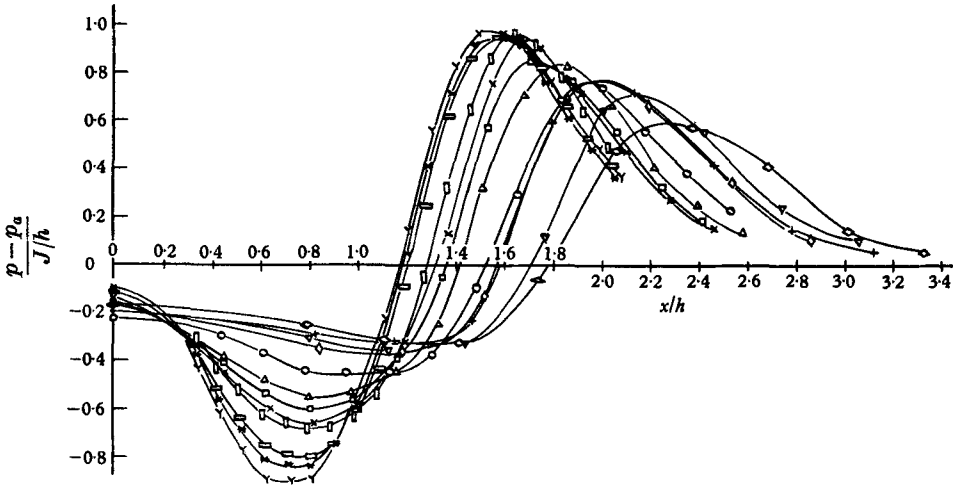

FIGURE 8. Static pressure distribution along the plate.

Symbol	h/t	Symbol	h/t
◇	4·15	□	9·13
▽	4·81	X	10·64
+	5·92	▯	10·65
◇	6·99	▭	14·06
○	5·62	*	16·74
△	7·35	Y	24·40

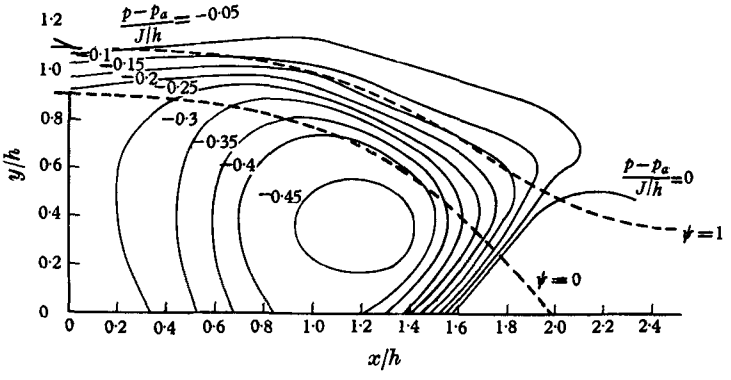

FIGURE 9. Static pressure contours for case $h/t = 5{\cdot}62$.

In the calculation it is necessary to assume a value of J, the jet momentum. It is found on integrating the calculated profiles that the values of the profile momentum are substantially larger than that at the slot exit, due to different static pressures at the various stations. The calculation has therefore been repeated using these new values of momentum at the relevant stations and the new

calculated profiles taken to be sufficiently close approximations to reality (they are almost identical with those originally found).

By comparing the values of jet momentum at the stations $x/h = 0{\cdot}609$, $1{\cdot}304$ with that measured at the jet exit, it is possible to obtain a check on the consistency of the Pitot and static tube measurements. It is found that the computed values of momentum agree to within 2%. This is of the same order as the uncertainty which exists regarding the use of Pitot and static tubes in highly fluctuating turbulent flows.

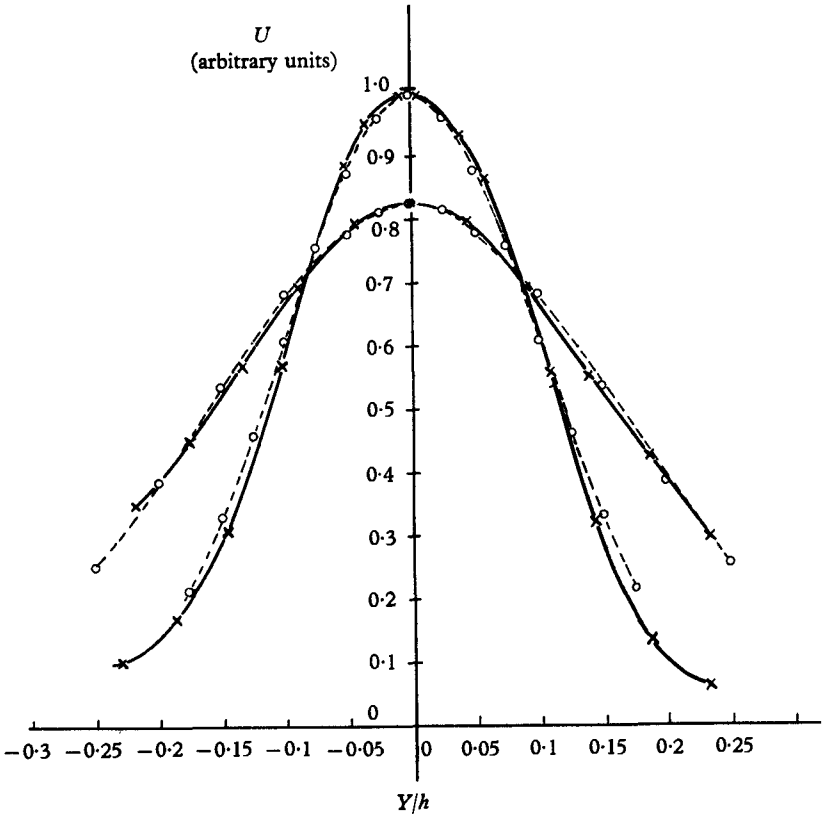

FIGURE 10. Jet profiles at $x/h = 0{\cdot}609$, $1{\cdot}304$ calculated from Pitot-static traverses by application of free-jet analysis with $\sigma = 15$. —×—, calculated profiles; –○–, plane jet profiles fitted to calculated profiles at U_{max} and $\frac{1}{2}U_{max}$.

In figure 10 the calculated jet profiles have been compared with the plane-jet profile as measured by Förthmann (1934) which has been matched at the values of $\overline{Y}/h$ corresponding to U_{max} and $\frac{1}{2}U_{max}$. There is quite close agreement between the curves. The profile at $x/h = 0{\cdot}609$ is somewhat flattened near $\overline{Y}/h$ for U_{max} but this is to be expected, for this station is only some 3·4 slot widths downstream of the jet exit. There is no indication of one-sidedness of the profiles expected from considerations of jet curvature.

It is possible to calculate an approximate value of σ, the spread parameter of the jet between these two profiles. Direct measurement of profile half-width

gives $\sigma = 9{\cdot}8$. Calculation based on velocity maxima gives $\sigma = 10{\cdot}3$ assuming $J/\rho U_0^2 h = 0{\cdot}191$, $\sigma = 11{\cdot}1$ assuming $J/\rho U_0^2 h = 0{\cdot}177$, $\sigma = 11{\cdot}9$ assuming $J/\rho U_0^2 h = 0{\cdot}165$ (i.e. that measured at the jet exit). Inasmuch as σ measures jet spread, a value in the region $\sigma = 10$ would be most realistic. It is noted that even taking the value of jet momentum to be that measured at the jet exit, the spread parameter is somewhat smaller than the value giving best agreement with the analysis. However, a reduced entrainment along the inner edge and an enhanced entrainment along the outer edge of the curved jet is expected to give a total spread parameter in the region of 10.

The analysis gives the volume of reversed flow:

$$\frac{Q_2}{U_0 h} = \frac{1-T_1}{2T_1}\sqrt{\left(\frac{J}{\rho U_0^2 h}\right)}\Big/\sqrt{\left(\frac{h}{t}\right)},$$

where $\cos\theta = \frac{3}{2}T_1 - \frac{1}{2}T_1^3$ and θ is the angle at which the jet strikes the plate. For $h/t = 5{\cdot}62$, $\sigma = 15$ and $J/\rho U_0^2 h = 0{\cdot}165$, $\theta = 43°$ and $Q_2/U_0 h = 0{\cdot}067$. Now the measured values are $\theta = 43°$ and $Q_2/U_0 h = 0{\cdot}068$, and so there is very good agreement in this case.

The reversed flow momentum J_2 is equal to $\frac{1}{2}J(1-\cos\theta)$ giving $J_2/J = 0{\cdot}135$ for $\theta = 43°$. The reversed flow momentum at $x/h = 1{\cdot}304$ is given by

$$J_2/\rho U_0^2 h = 0{\cdot}021,$$

at $x/h = 0{\cdot}957$ is $J_2/\rho U_0^2 h = 0{\cdot}018$

by integration of velocity profiles, so that at $x/h = 1{\cdot}304$ and $0{\cdot}957$, $J_2/J = 0{\cdot}127$ and $0{\cdot}109$. Again there is good agreement with the analysis.

The pressure recovery experienced by the reversed flow is given by $\Delta p_2/(J/h) = 0{\cdot}23$ from figure 8. This corresponds to the case of a jet with momentum J_2 entering a rectangular control volume through one end, losing this momentum entirely in a pressure rise and diffusing sideways out of the control volume. The pressure difference Δp_2 across the control volume is given by $h_0 \Delta p_2 = J_2$, so that $h_0/h = (J_2/J)\,\Delta p/(J/h)$. If $\Delta p_2/(J/h) = 0{\cdot}23$, $J_2/J = 0{\cdot}132$ then $h_0/h = 0{\cdot}57$. This is of the order expected, for if a control volume is constructed which is bounded by the plate, the step, the station $x/h = 1{\cdot}2$, and the locus of points at which the component of mean velocity parallel to the plate is zero, integrating the pressure round the control volume gives the loss of momentum in the x-direction. The shape of such a control volume is expected to be a function of the shape of the cavity. Values of h_0/h have been calculated as follows. For each measurement a mean value of σ from figures 6 and 7 is obtained, which with the known value of h/t gives the value of θ relevant to the analysis. Writing $J_2/J = \frac{1}{2}(1-\cos\theta)$ and using the experimental results of pressure recovery gives h_0/h from the above relation. In figure 11 h_0/h is plotted against θ. It is seen that the points lie on a reasonably well-defined curve for larger values of θ (i.e. for larger h/t). With this information it is possible to predict the back pressure on the step by the analysis.

Table 4 gives values of total pressure at stations on the reattaching streamline and on the locus of positions at which the velocity of the y-wise profiles is a maximum. It is interesting to see that the values of streamline number ψ for the positions of $U_{\max}$ on the y-wise profiles are very near to $0{\cdot}5$ for a considerable

distance along the curved jet. The effect of non-uniformity of the jet profile at the slot is very quickly lost, and any expectation of a clearly defined upwards trend of $\psi_{U_{\max}}$ with x/h which, in the absence of one-sided profiles, would perhaps reflect different mixing rates on the two sides of the jet, has not been fulfilled. Figure 8 shows that the maximum pressure on the plate $(p-p_a)/(J/h) = 0{\cdot}77$ is

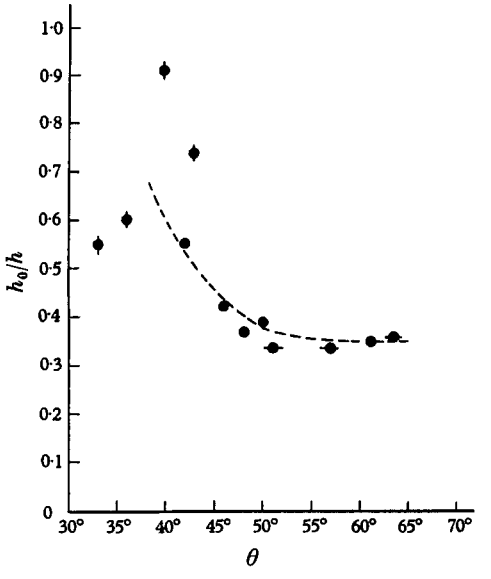

FIGURE 11. Pressure recovery parameter. ϕ, ½ in. step; ●, 1 in. step; ⊸, 2 in. step.

x/h	$(y/h)_{\psi=0}$	$\left(\frac{\frac{1}{2}\rho u^2}{J/h}\right)_{\psi=0}$	$\left(\frac{P-p_a}{J/h}\right)_{\psi=0}$
0·609	0·870	1·41	1·13
0·957	0·780	1·35	0·975
1·304	0·620	1·08	0·67
1·652	0·355	0·725	0·46

x/h	$(y/h)_{U_{\max}}$	$\frac{\frac{1}{2}\rho U_{\max}^2}{J/h}$	$\left(\frac{P-p_a}{J/h}\right)_{U_{\max}}$	$\psi_{U_{\max}}$
0·609	0·955	3·11	2·92	0·47
0·957	0·885	2·92	2·62	0·47
1·304	0·760	2·58	2·29	0·50
1·652	0·575	2·26	2·03	0·63

TABLE 4. Total pressures on reattaching streamline and locus of velocity maximum of y-wise profiles. For case $h/t = 5{\cdot}62$.

much higher than that obtained by extrapolating the total pressure on the reattaching streamline, but is very much lower than that obtained by extrapolating the total pressure on the maximum velocity locus. This can be explained by considering the effect of a highly fluctuating flow near the reattachment point; the high-velocity parcels of fluid give a correspondingly larger contribution to the wall pressure than the lower-velocity parcels. Streamlines depend on mean squared velocity.

8. Conclusions

The variations of $\Delta p/(J/h)$ and l/h with h/t found experimentally agree quite closely with those predicted by the Dodds analysis (as amended by Bourque) in that they are consistent with a choice of spread parameter σ which is substantially constant at the value 15 over the range of $h/t > 6$. The relevant value of σ is somewhat larger than this for h/t in the region of 4.

Detailed flow measurements for the case $h/t = 5{\cdot}62$ show that $\sigma = 15$ gives reasonably accurate prediction of initial reversed volume flow and reversed flow momentum.

The value of σ for which the analysis is in best agreement with the results is not in fact the true value of the spread parameter for the curved jet, and the discrepancy between the two values is a measure of the collective errors in the various assumptions made in the analysis, so that the choice of $\sigma = 15$ is now to be regarded as the fixing of a convenient empirical constant in order that the analysis may be applied to give reasonably accurate predictions of cavity length and cavity pressure. In this connexion it is noted that any change in the rate of entrainment along the inner and outer edges of the jet due to curvature effects as predicted by momentum transport considerations, would not necessarily be accompanied by a change in the rate of growth of the jet as a whole. Since the velocity profiles across the curved jet were found to be very like those of a plane jet, a difference in the rate of entrainment on the two sides of the jet would imply that the locus of velocity maximum is not a streamline. The measurements of velocity and pressure are not of sufficient accuracy to detect this effect and further experiments are being carried out to investigate the effect of curvature on entrainment properties.

The author wishes to thank Dr M. R. Head for his advice and encouragement, and also Mr H. Bridgeman who constructed the apparatus.

REFERENCES

BOURQUE, C. 1959 M.Sc. Thesis. University of Laval. Also *Aero. Quart.* **11**, 201.

CORRSIN, S. & KISTLER, A. L. 1954 The free-stream boundaries of turbulent flows. *NACA Tech. Note* 3133.

DODDS, J. I. 1960 Ph.D. Thesis. Cambridge University.

FÖRTHMANN, E. 1934 Über turbulente Strahlausbreitung. *Ingen.-Arch.* **5**, 42. Also *NACA Tech. Note* 789.

GÖRTLER, H. 1942. Berechnung von Aufgaben der Freien Turbulenz auf Grund eines neuen Näherungsansatzes. *Z. angew. Math. Mech.* **22**, 244.

HEAD, M. R. 1958 Entrainment in the turbulent boundary layer. *A.R.C. Report* no. 20,338.

LUDWIEG, H. & TILLMAN, W. 1951 Investigations of the wall-shearing stress in turbulent boundary layers. *NACA Tech. Mem.* 1285.

MILLER, D. R. & COMINGS, E. W. 1960 *J. Fluid Mech.* **7**, 237.

REICHARDT, H. 1942 Gesetzmässigkeiten der freien Turbulenz. *VDI-Forschungsheft*, p. 414.

TOWNSEND, A. A. 1956 *The Structure of Turbulent Shear Flow.* Cambridge University Press.

YOUNG, A. D. & MAAS, J. N. 1936. The behaviour of a Pitot tube in a transverse total-pressure gradient. *A.R.C. Rep. & Mem.* no. 1770.

Appendix

Calculation of jet profiles from profiles in the y-direction

The notation is shown in figure 12. The velocity at $\bar{y}$ is that corresponding to $(X, Y) = (\bar{X} - \bar{y}\sin\phi, \bar{y}\cos\phi)$, i.e. to

$$\bar{\eta} = \frac{\sigma\bar{y}\cos\phi}{\bar{X} - \bar{y}\sin\phi}, \quad X = \bar{X} - \bar{y}\sin\phi.$$

Hence
$$\frac{(u)_{\bar{y}}}{(U_{\max})_{\bar{X}-\bar{y}\sin\phi}} = \operatorname{sech}^2\bar{\eta} = \left(\frac{u}{U_{\max}}\right)_{\bar{X},\bar{Y}}, \tag{1}$$

which defines $\bar{Y}$ to be the Y-co-ordinate of the required profile corresponding to $\bar{\eta}$, and so corresponding to $\bar{y}$ of the measured profile. Therefore

$$\frac{\sigma\bar{y}\cos\phi}{\bar{X} - \bar{y}\sin\phi} = \bar{\eta} = \frac{\sigma\bar{Y}}{\bar{X}},$$

and hence
$$\bar{Y} = \bar{y}\cos\phi\,\frac{\bar{X}}{\bar{X} - \bar{y}\sin\phi}. \tag{2}$$

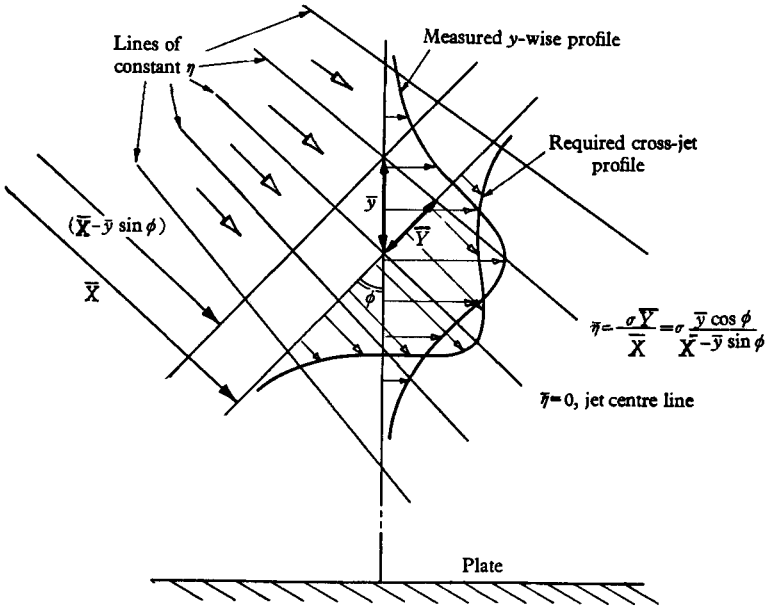

FIGURE 12. Notation used in appendix.

Now from (1), $$\left(\frac{u}{U_0}\right)_{\bar{X},\bar{Y}} = \left(\frac{u}{U_0}\right)_{\bar{X}-\bar{y}\sin\phi,\,\bar{y}\cos\phi} \frac{(U_{\max})_{\bar{X}}}{(U_{\max})_{\bar{X}-\bar{y}\sin\phi}},$$

and so
$$\left(\frac{u}{U_0}\right)_{\bar{X},\bar{Y}} = \left(\frac{u}{U_0}\right)_{\bar{X}-\bar{y}\sin\phi,\,\bar{y}\cos\phi} \sqrt{\left(\frac{\bar{X} - \bar{y}\sin\phi}{\bar{X}}\right)}, \tag{3}$$

for free-jet analysis gives
$$J = \tfrac{4}{3}\rho U_{\max}^2 \frac{X}{\sigma}.$$

Now
$$\frac{\bar{X}}{h} = \tfrac{3}{4}\sigma \left(\frac{J}{\rho U_0^2 h}\right) \left(\frac{U_0}{U_{\max}}\right)_{\bar{X}}^2. \tag{4}$$

Equations (2) to (4) then give the required profile. Intitially $J/\rho U_0^2 h = 0{\cdot}165$, as measured at the jet exit.

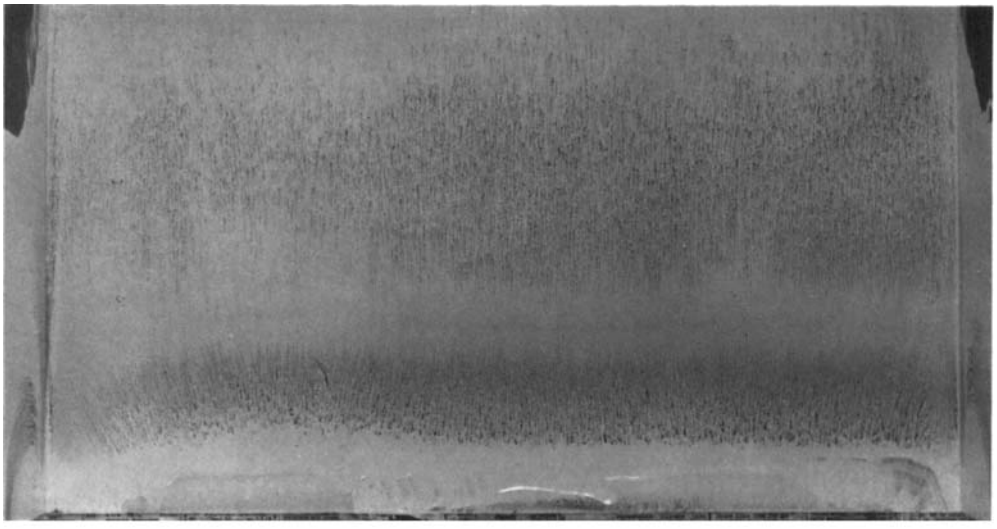

(*a*)

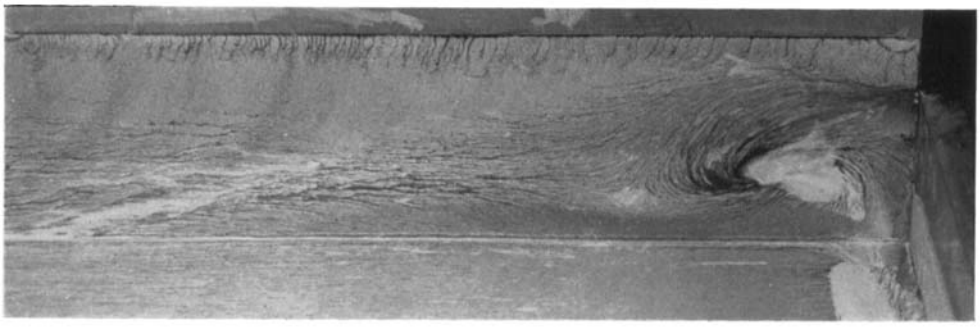

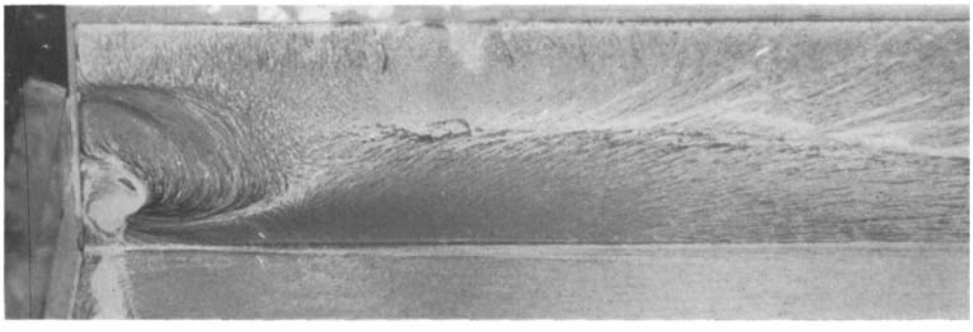

(*b*)

FIGURE 3 (plate 1). Flow visualization of surface streamlines.
(*a*) Base plate; (*b*) end-plates.